

# Effects of the micro surface texturing in lubricated non-conformal point contacts

<sup>1,2</sup>G.S. Joshi, <sup>1,2</sup>C. Putignano, <sup>1</sup>C. Gaudio, <sup>3</sup>T. Stark, <sup>3</sup>T. Kiedrowski, <sup>1</sup>A. Ancona, <sup>1,2</sup>G. Carbone\*

<sup>1</sup>CNR – Institute for Photonics and Nanotechnologies U.O.S. Bari, Physics Department “M. Merlin”, via Amendola 173, I-70126 Bari, Italy.

<sup>2</sup>Politecnico di Bari, Department of Mechanics, Mathematics and Management, V.le Japigia 182, I-70126 Bari, Italy .

<sup>3</sup>Robert Bosch GmbH, Corporate Research, Robert-Bosch-Campus 1, 71272, Renningen, Germany.

## Abstract

This paper presents an experimental study on the effects of micro-textured surfaces on lubricated non-conformal point contacts. Thus, we focus on a regime poorly investigated in literature, where the contact area and the micro-holes have a comparable size. Tribological characterization are performed on three geometrical patterns, which are textured on stainless steel polished surfaces. Experiments are carried out on a rheometer, where a steel ball slides against the surface of the samples. These samples are tested with two different viscosities of the PAO (Poly-Alpha-Olefin) as a lubricant. Results show the change in the friction with respect to the sliding velocity under different lubrication regimes due to the stress, void ratio and two different kinematic viscosities of PAO. In particular, we show that, depending on the void ratio, a significant friction reduction or, on the contrary, a deterioration of the frictional performances can affect the boundary and mixed lubrication regimes. This is due to the simultaneous occurrence of two competing effects. One is related to the stress intensification, due to the presence of the micro-hole edges on the contact topography, which leads to a consequent increase in wear and friction. On the other hand, micro-texture may play a positive role in the friction optimization given the possibility, offered by the micro-holes, to entrap wear debris and, then, to preverse a smoother interface between the contacting pairs.

**Keywords:** Surface Texturing, femtosecond laser ablation, lubrication, non-conformal, friction.

\* Corresponding author. Tel.: +39 366 241 3100

*E-mail address:* gagandeepsingh.joshi@ifn.cnr.it

## 1. Introduction

Topography of the surfaces plays important role in influencing the tribological properties of the materials and, in particular, the friction behavior of the two-rubbing surfaces during conformal and non-conformal contacts. Different research groups around the globe are trying to understand the complex behavior of the tribological properties, in terms of friction and wear, in order to improve the efficiency and to increase the life time of the mechanical systems or components [1]. Over the past decades, surface texturing has shown to be an emerging technique to control the friction and wear. It consists of fabricating a pattern of small dimples or grooves on the surface of the materials in a very controllable way, which causes the change in the surface topography. In an engineering setting, the concept of "micro-irregularities" was first introduced by Hamilton and Allen in 1966 [2], [3]. They pointed out that

by adding "asperities and depressions" to one face of a parallel rotary-shaft face seal, the load support capabilities of the seal could be improved. Various techniques can be employed for surface texturing, which includes vibro-rolling (Schneider- 1984) [4], reactive ion etching (Wang-2003) [5] and Laser Surface Texturing (LST) (Etison-1996) [6], but the latter is probably the most advanced so far. LST is a process that can generate periodic micro or nano or hierarchical micro/nano structures involving very thin layer of material surface by laser ablation. The generated micro- dimples can serve either as a micro-hydrodynamic bearing in cases of full film lubrication or mixed lubrication, a micro-reservoir for lubricant in cases of starved lubrication conditions, or a micro-trap for wear debris in either lubricated or dry sliding [7,8]. So, if properly designed, the macroscopic effect of such micro structuring is an enhancement of the load capacity, wear resistance, and friction properties of the laser-treated surfaces. Recently,

Gachot et al. summarized the effects of surface textures under the operative lubrication regimes in the Stribeck curve, with a clear distinction between conformal- and non-conformal contact [9]. For the latter case, the reader is also referred to [10]. Over the past 20 years, a lot of research have been conducted and reported as studies on surface texturing, covering both experimental and theoretical investigations. In this regard, Gropper et al. presented a comprehensive review article with a focus on the different modeling techniques and numerical methods commonly used to predict the performance of textured or rough surfaces [11].

Nowadays, LST with femtosecond pulses, in particular, has emerged as a potential new technology to reduce friction in mechanical components. Texturing can be done with different laser systems, but femtosecond laser seems to be more beneficial as compared to the other laser sources [12]. The advantages of using femtosecond laser pulses compared to nanosecond ones reside in the fact that the ablation process is substantially melting free. Therefore, no pile-up of the material at the edges of the micro-dimples, which could be detrimental to the desired tribological behavior, and no further polishing of the surfaces is required after the laser treatment. Furthermore, femtosecond laser ablation allows fine control of the geometry of the dimples with micrometer precision [13]. The benefit arising from micro surface texturing including the micro-cavities or grooves on a flat surface is a combination of several effects, which improve oil supply and reduced abrasion in the sliding contact. In a recent study, Vladescu et al. showed that pockets act to reduce monotonically both friction and wear as the sum of the pocket volumes passing through contact increases. The study showed that individual pocket width and depth values can largely be ignored, so long as the overall volume of a pocket is maximized [14,15,16]. This is indeed consistent with what Varenberg et al. showed about the proposed mechanism of wear debris entrapment in Ref. [17]. As a further contribution to the field, it is interesting to recall the investigation, carried out by Rosenkranz et al., on the effect of hemispherical dimples produced by micro-coining on the tribological behaviour under mixed and full film EHL lubrication. They showed that the coined surfaces with higher densities and depths is more likely to induce cavitation. As a consequence, the load bearing capacity of these

samples is reduced and no reduction or even an increase in the coefficient of friction can be observed [18]. In this regard, it is interesting to observe that, conversely, according to Krupka et al., surface texturing could represent the way how to increase lubrication efficiency of rolling/sliding non-conformal contacts under transient operational conditions through the lubricant emitted from micro-dents. They showed that the lubricant emitted from the micro-dents helps to separate rubbing surfaces especially under thin film lubrication conditions, where the rubbing surfaces move in the opposite direction [19]. When surface irregularities appear at sufficient density, they can improve the wetting of the surface by an oil [20,4], and thereby support the lubricating oil film formation. At higher sliding speed, and with a sufficient supply of oil, individual surface cavities may act as hydrodynamic pressure pockets, which reduce friction, unless the benefit is counteracted by turbulence effects. Recent investigations have shown that, in this regime, also cavitation in the holes can play an important role, by decreasing the viscous losses and, then, the total friction [5]. Finally, it should be noticed that a drawback of the surface irregularities may occur as abrasive wear of a soft counter surface at high contact pressure [21].

Moving from this context, our work focuses on a topic only partially enlightened in literature: this is the tribological performances of the micro-textured surfaces during non-conformal point contacts under lubricated conditions. As mentioned before, the largest part of theoretical and experimental analyses have investigated conformal contact conditions, where the contact area is much larger than the pocket size. In this study, we wonder what happens, in terms of friction, when the contact region has a width comparable with the hole diameter. Indeed, such conditions are significant in a variety of applications, involving conformal point contacts, such as in ball bearings. Here, different tests are performed to study the tribological effects, which arise due to the contact length or contact pressure (stress) and the void coverage factor. These tests are performed by using a lubricant of two different viscosities from PAO (Poly-Alpha-Olefin). We show how, depending on the properties of the texture and, specifically, on its void ratio, i.e. the ratio between the portion of surface occupied by the micro-holes and the entire surface of the samples, the tribological properties

may change very differently. This is qualitatively discussed in the paper observing how different and competitive mechanisms occur when a texture pattern is introduced: their interplay may result in an improvement or, conversely, in a deterioration of the friction performance. Ultimately, the paper shows how, in comparison with conformal contact

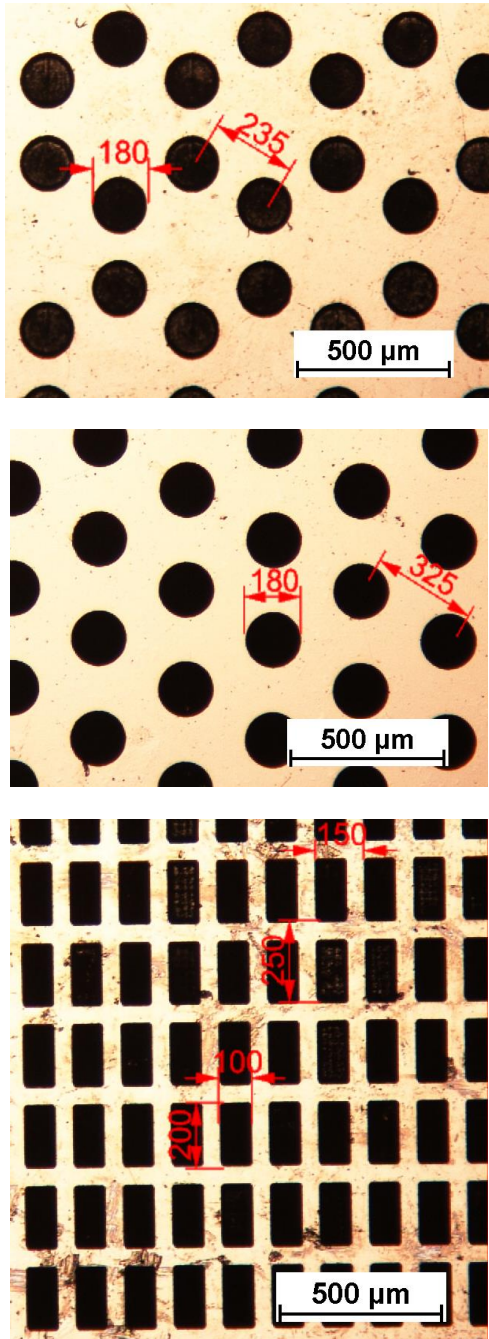


Figure 1: Micro-textured geometries for the circular (hexagonal and triangular patterns) and the rectangular dimples. All the quotes are expressed in micrometers.

mechanics, textured interfaces in point contacts may behave very differently, thus demonstrating the necessity of more experimental and theoretical investigations in the field.

## 2. Experimental Setup

### 2.1 Surface texture manufacturing by Femtosecond laser ablation process (fsLA)

The surface of the samples has been micro-textured with three different geometrical patterns as shown in Figure 1, where we report all quotes characterizing the three textures. Specifically, we have fabricated an exagonal and a triangular pattern, both with circular dimples, and a rectangular one with rectangular dimples. The micro surface texturing has been performed upon stainless steel (1.4112) samples, having a surface roughness of 0.2  $\mu\text{m}$ . Fabrication has been done by using a scanner interfaced ultrafast fiber CPA laser system (mod. Sci-series from Active Fiber Systems GmbH), delivering 650 fs pulses at a wavelength of 1030 nm, with repetition rate ranging from 50 kHz to 10 MHz, maximum pulse energy of 100  $\mu\text{J}$  and maximum average power of 50 W. After passing through a beam expander, the laser beam has been guided to the galvo-scanner (Hurryscan from ScanLab GmbH) head, equipped with a 100- mm focal length F-Theta lens. The resulting laser beam spot size on the sample surface  $2w_0$  was about 25  $\mu\text{m}$ .

Types of textured geometry	Void ratio (%)	Speed (mm/s)	Hatch Type	Track depth ( $\mu\text{m}$ )
Hexagonal	27	22	Concentric	6.6
Triangular	29	34	Concentric	6.7
Rectangular	53	50	Crossed, Horizontal and Vertical	7.3

Table 1. Process parameters defined for each texture geometry. [circular dimples textured in

hexagonal and triangular lattice, quasi rectangles textured in rectangular lattice]

The laser has been operated at a repetition rate  $f$  of 50kHz, with an average power  $P$  between 60 and 70 mW. Therefore, the laser fluence, determined as  $F = \frac{2E}{\pi w_0^2}$ , where  $E$  is the pulse energy, was between 0.49 and 0.57 J/cm<sup>2</sup>. For the three different textured geometries, different milling strategies have been used. For both the hexagonal and triangular texturing, the dimples have been generated by moving the laser beam along concentric circles, with a hatch distance of a few micrometers and a speed of 22 mm/s and 34 mm/s, respectively. For the rectangular geometry, crossed horizontal and vertical milling hatches have been performed at 50 mm/s. In these irradiation conditions, the number of pulses overlapping on the same focal area was determined as  $N = \frac{2w_0 f}{v}$  and resulted between 25 and 57. The threshold fluence ranged from 0.16 J/cm<sup>2</sup> to 0.15 J/cm<sup>2</sup>. It was calculated starting with the single pulse threshold fluence ( $F_{th}(1) = 0.21$  J/cm<sup>2</sup>) and the incubation coefficient factor ( $S = 0.91$ ) values found in the literature [22, 23] and using the Jee incubation model [24] in order to take into account the reduction of the ablation threshold due to the irradiation with multiple pulses,. Therefore, laser ablation was performed nearly above the threshold fluence, in order to achieve a high level of accuracy and reproducibility of the machined microstructures. The desired dimples depth was achieved by finely adjusting the number of overlapped loops. The main process parameters are summarized in Table 1.

## 2.2. Characterization

The tribological properties of the micro-textured samples were evaluated by using different apparatus. The rheometer MCR-301 was used as a tribometer to perform the friction test under a normal force of 20 N at 25°C. The setup is based on the ball-on-three-plates-principle (or-ball-on-pyramid) consisting of a a steel ball holder, an inset where three small plates can be placed, and a bottom stage movable in all directions on which the inset can be fixed. Figure 2 depicts the setup schematically. The ball fixture enables the use of balls made of different materials, and their easy replacement. The plate texture at the bottom part is mounted on a special designed spring system

allowing motion in all directions of the coordinate system:  $x$ ,  $y$ ,  $z$ . This flexibility ensures the concentric positioning of the fixture to achieve a uniform force distribution from the ball onto all the three plates. The rotational speed applied to the shaft is producing a sliding speed of the ball with respect to the plates at the contact points. The resulting torque can be correlated with the friction force by employing simple geometric calculations. The normal force  $F_N$  of the rheometer is transferred into a normal load  $F_L$  acting perpendicular to the bottom plates at the contact points. We have, then, the following relations:

$$F_L = (1/3) \cdot \sin\alpha \cdot F_N$$

with  $r_{ball}$  being the radius of sphere and  $\alpha$  the angle of the plates, respectively. In the specific configuration employed in the apparatus, we employ  $\alpha = \pi/4$ , a ball with a radius  $r_{ball} = 6.35$ mm, a force  $F_N = 20$ N; thus,  $F_L$  is equal to  $F_L = 4.71$  N.

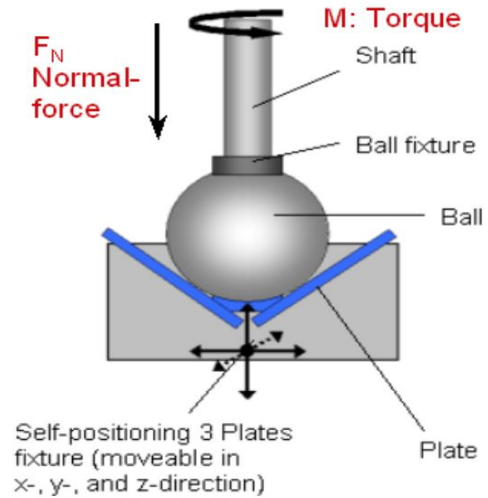


**Figure 2:** Schematic representation of the ball on three-plates-device

Given such a configuration, by means of the classic Hertzian relations, we can estimate the contact diameter as  $D = 115.8$   $\mu$ m. We observe that, indeed, such a value is comparable with the characteristic dimensions of the dimples.

With regards to the experiments, before carrying out the friction tests, the tribopairs have been ultrasonically cleaned using isopropanol, followed

by rinsing with Petrolether and air dried. Experiments have been performed under pure sliding conditions by using a steel ball (100 Cr6, G-28) within the sliding range, which varies from 0.0001m/s to 1.4m/s. The samples with different geometrical patterns have been aligned parallel to the ball sliding direction. In detail, in the case of the rectangular dimples, we have aligned the longer axis with the sliding velocity of the ball. Whereas, in the case of the hexagonal and triangular geometrical patterns, given the circular dimples, the textures are perfectly isotropic and, thus, there is no preferential direction for the alignment.

As for the experimental setup, a fixed quantity of lubricant, i.e. 1 $\mu$ l poly-alpha-olefin without additives (base oil: Isoflex Topas L32), whose properties are included in Table 2, was distributed on each plate at the point of the tribo-contact with  $\mu$ -Pipette during each test and a new ball was used for each test. In each measurement cycle, three identically textured samples are placed in the sample holder and are tested. The measurement cycle can be divided into two different regimes. The first regime is the endurance part in which the rotational speed is kept constant at 20 rpm and the load is equal to 20 N. The second regime is the so-called Stribeck part in which the load  $F_N$  is kept constant at 20 N but the rotational speed is ramped up from 0 to 3000 rpm in a logarithmic way. This ramp-up is repeated three times within one Stribeck part. Both regimes occur twice. The first endurance part takes 45 minutes and is carried out in order to avoid any transient effect, due to a running-in behavior, when recording the first set of Stribeck curves. Indeed, after this first Stribeck package, including three curve measurements, a second endurance part is run for another 60 minutes. In the end, the Stribeck part with three curve measurements is repeated. Therefore, for each measurement cycle we obtained six Stribeck curves which were averaged in the result plots.

Finally, the morphologies of the surfaces have been characterized by using LEXT OLS4000-Industrial Laser Confocal Microscopes 3D and Leica DM4000 M for Material Analysis. Contact pressure measurements have been performed with Fujifilm pressure measurement foils. The foils have been positioned in the contact area and glued to the tested samples .

**Table 2:** Viscometric Characteristic

<b>Low Viscosity Lubricant</b> (Type 1-Poly-alpha-olefin)	39.5 mm <sup>2</sup> /s at 20°C
<b>High Viscosity Lubricant</b> (Type 3-Poly-alpha-olefin)	1300 mm <sup>2</sup> /s at 40°C

Pressure measurement tests have been carried out under a load equal to  $F_L = 20$  N, applied on the steel ball, without lubricant in a static condition for 10 minutes. After each test, the area of the contact pressure has been examined by using Leica DM4000 Microscope and Fujifilm Pressure Distribution Mapping system (FPD-8010E).

### 3. Results and Discussion

Preliminary pressure measurement tests have been conducted to visualize the differences, in terms of stress distribution, between the textured and the un-textured samples. Indeed, the contact pressure plays a crucial role in determining the wear ratio and, consequently, the friction [14-16].

In detail, foils have been tested with both textured and un-textured samples under the same conditions and, later, analyzed by using Leica DM4000 microscope. Depending on level of the red colour (see insets of Figure 3), and by employing the Fujifilm Pressure Distribution Mapping system (FPD-8010E), it is possible to obtain in each point an estimation of the pressure value. Being the technique based on the qualitative evaluation of the images of the measurement foil, the pressure results plotted in Figure 3 have to be considered indicative, but, at the same time, they provide significant information on how the surface topography influences the pressure distribution. The dark red spots noticed in the insets of Figure 3 indicate the area effected by a high applied pressure (stress), whereas the light red spots represent the contact zone under an area of low pressure or stress. Incidentally, we notice that these values are consistent with the dimensions previously calculated from the Hertzian theory.

More in detail, in Figure 3, we focus on the contact pressure distributions in two cases: the first one refers to the un-textured samples, whereas the second one is obtained testing the rectangular textured pattern. In spite of the rough

estimations offered by the pressure sensitive foils, we observe quite clearly that the micro-texture produces a significant increase of the pressure distribution. This is due to the presence of the micro-holes edges which, ultimately, act as stress intensity factors [25, 26]. Such an effect seems crucial in non-conformal contacts where the contact area is comparable with the pocket size. Indeed, in Figure 4, confocal images for the rectangular geometry (on the top) and for the hexagonal pattern (on the bottom) show that the worn zone has the same size of the one rectangular micro-hole or pocket.

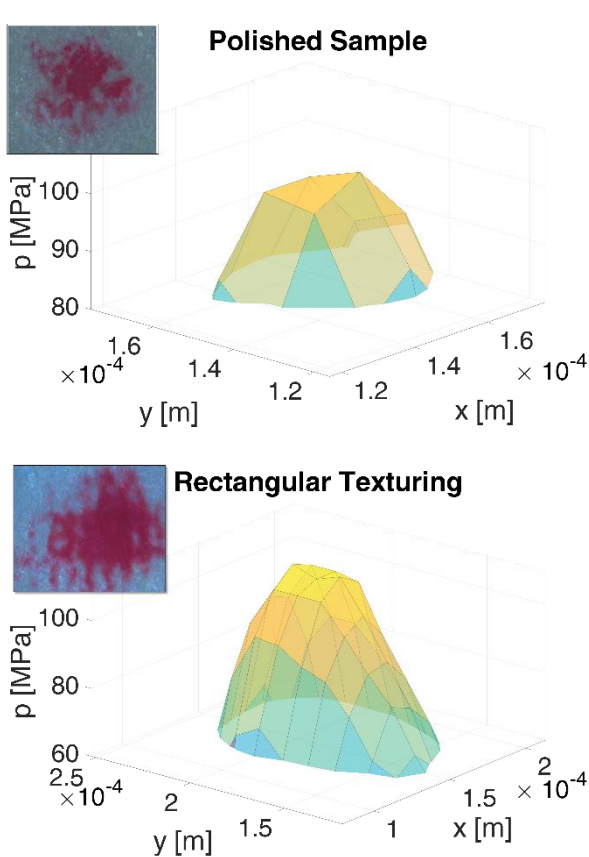


**Figure 3:** Contact pressure distribution maps (FPD-8010E) based on the analysis of the acquired microscope images of the Fujifilm measurement foils shown in the insets.

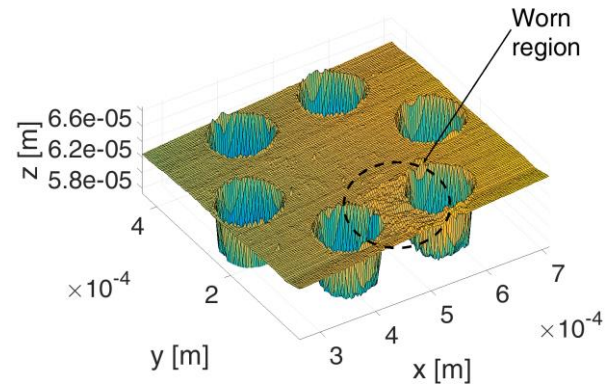
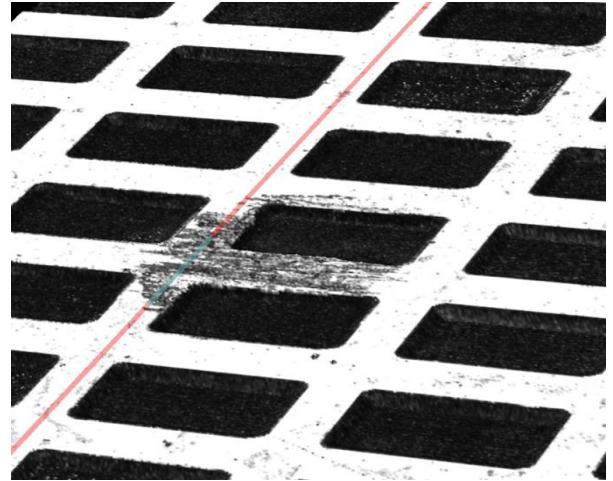


**Figure 4:** Industrial Laser Confocal Microscope 3D Images(50X) for the rectangular geometry texture (*on the top*) and CSM Confocal Microscope Images for the hexagonal texturing (*on the bottom*). In both cases, the worn zone is clear.

The higher pressure due to the presence of the micro-texture is a potential evidence of larger wear. This is particularly critical in all the regimes where we do not have a fully developed lubrication film and where, as a consequence, the wear ratio tends to be higher. Larger wear implicates larger friction, and, therefore, the presence of a micro-pattern seems to be detrimental in conformal contacts [16]. However, the presence of micro-holes may play also a positive role. Indeed, in the mixed and boundary regimes, where the wear is larger, the holes constitute an opportunity to entrap the debris and, therefore, to contribute to have a smoother interface between the contacting bodies [15]. This may entail the reduction of the interfacial

friction. Ultimately, in the presence of micro-textured surfaces in point non-conformal contacts, two competitive mechanisms can be expected: on one side, the presence of the holes edges produces an intensification of the stress distribution and, therefore, an increase of the wear ratio; on the other hand, the holes can capture the debris related to the wear process and, therefore, can help in obtaining a smoother interface and, ultimately, a smaller friction force.

All this is confirmed in Figure 5, where we plot the friction coefficient,  $\mu$ , as a function of the sliding velocity,  $u$ . Each micro-texture geometry has been tested under the same conditions by using two different lubricants (shown in Table. 2). In both cases, we focus on the mixed and boundary regimes, where it is well known that the wear plays a fundamental role and, consequently, it is more interesting to investigate the effects of a textured pattern. In Figure 5a and 5b, we observe that, in comparison with the results of the untextured samples, the hexagonal and the triangular patterns produce a deterioration of the frictional performances, whereas the rectangular pattern shows an improvement in the order of 20%. Interestingly, these two opposite trends look stronger at low speed, where the wear is expected to be larger. The different behavior can be explained by assuming that the two aforementioned mechanisms, both related to the wear, intervene differently in the two cases. Indeed, for the triangular and the hexagonal lattices, the wear increase, related to the change in the topography, prevails and determines an increase of the friction force. Conversely, in the case of the rectangular micro-holes, the debris entrapment effect seems to dominate and determines, in the mixed and the boundary lubrication regimes, a reduction of the frictional losses. As the first process, i.e. the stress intensification and, consequently, the larger wear, cannot depend significantly on the dimple geometry since it is mainly related to the presence of sharp edges in the contact region, the very different experimental outcomes have to be related to the second mechanism, i.e. the debris entrapment, which is strictly dependent on its turn on the void ratio. Indeed, a larger fraction of dimples on the total sample surface can guarantee more space, for the wear particles, to be captured in the micro-holes. This is what occurs in our case where the rectangular pattern, with a void ratio of

53%, performs much better than the other two cases.

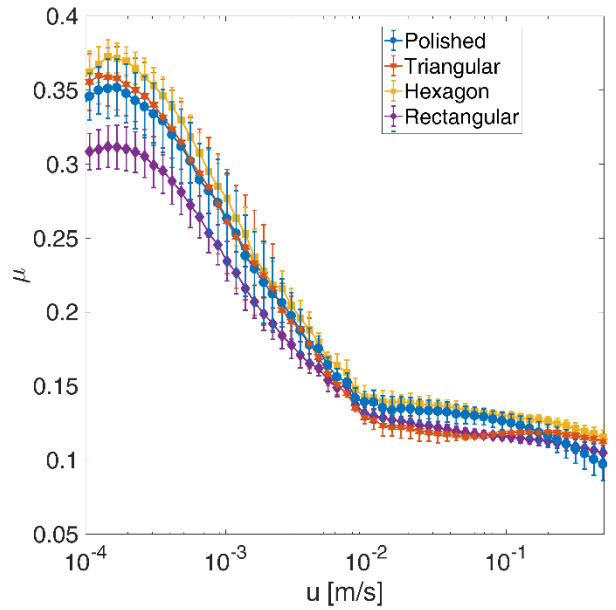


Fig. 5(a)

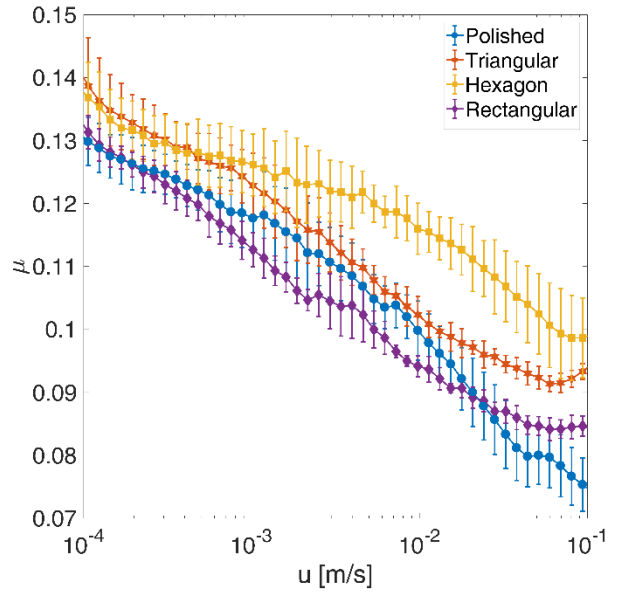


Fig.5(b)

**Figure 5:** Friction coefficient,  $\mu$ , vs. sliding velocity,  $u$ . Figure 5a and 5b refer respectively to the low viscosity (Type 1) and the high viscosity lubricant (Type 3). For each measure, we report the scatter as an errorbar.

We can conclude that, in the occurrence of conformal contacts, the presence of a micro-textured surface can have different consequences, depending on the effect that ultimately prevails,

i.e. the wear increase or the debris entrapment. The latter seems related to an increased void ratio.

#### 4 Conclusions

This paper deals with the study of the micro-textured effects in non-conformal lubricated point contacts. Large research efforts have been dedicated to analyze the texture performance in presence of conformal contact mechanics [9,15], but a little has been told about what occurs when the contact area has the same size of the textures holes, as in any non-conformal contacts.

In this paper, we focus on this last case and show that introducing a surface texture may have opposed outcomes. Indeed, in comparison with un-textured samples, it can bring to a deterioration of the frictional performances, but, on the other hand, can also determine a significant reduction of the frictional losses. This has been related to the occurrence of two different competing mechanisms: one deals with the stress intensification provoked by the holes edges, which contribute to intensify the stress, thus increasing the wear ratio and, therefore, the friction losses. The other element is related to the debris particles entrapment, to the creation of a smoother interface and, consequently, to a reduced friction. Depending on the mechanism which prevails, the texture introduction can worsen or improve the tribological performances. Our tests show that a high void ratio can be useful to enhance the entrapping effect and decrease the friction. Ultimately, the paper points out the necessity to pay more attention to the micro-texture in conformal contacts as a tool to optimize friction.

#### Acknowledgements

The authors acknowledge the National Research Council of Italy and European Commission for having supported the research activity within the project "Laser4Fun", which is funded under the European Union's Horizon 2020 research and innovation programme under the Marie Skłodowska-Curie grant agreement No. 675063.

#### References

[1] The use of anisotropic texturing for control of directional friction; P Lu, R.J.K. Wood, M.G. Gee, L. Wang, W. Pfleging, "Tribology International" vol 113, pg 169, (2017)

[2] A Theory of Lubrication by Microirregularities; D. B. Hamilton, J. A. Walowit, and C. M. Allen, "Trans. ASME J. Basic Eng." vol. 88, pg 177, (1966)

[3] Microasperity Lubrication; J. N. Anno, J. A. Walowit, and C. M. Allen; "J. Lubr. Technol." vol. 90, no. 2, pg 351, (1968)

[4] Efficiency of laser surface texturing in the reduction of friction under mixed lubrication; D. Braun, C. Greiner, J. Schneider, P. Gumbsch; "Tribology International" vol 77, pg 142, (2014)

[5] The Transient Friction Response of a Laser-Textured, Reciprocating Contact to the Entrapment of Individual Pockets ;SC. Vladescu, S. Medina, AV. Olver, IG. Pegg , T. Reddyhoff ; "Tribol Lett" vol 62, pg 19, (2016)

[6] Friction Properties of Lubricated Laser-MicroTextured-Surfaces: An Experimental Study from Boundary- to Hydrodynamic-Lubrication ; M. Scaraggi, F.P. Mezzapesa, G. Carbone, A. Ancona, L. Tricarico; "Tribol Lett" vol 49, pg 117, (2013)

[7] Effect of surface topography on mixed lubrication film formation during start up under rolling/sliding conditions; I. Krupka , P. Svoboda, M. Hartl; "Tribology International" vol 43, pg 1035, (2010)

[8] Minimize friction of lubricated lasermicrotextured-surfaces by tuning micro holes depth; M. Scaraggi , F.P. Mezzapesa , G. Carbone, A. Ancona, D. Sorgente, P. M. Lugarà, "Tribology International" vol 75, pg 123, (2014)

[9] A critical assessment of surface texturing for friction and wear improvement ;C. Gachota, A. Rosenkranz , S.M. Hsu , H.L. Costa, "Wear" vol 372–373, 15 pg 21, (2017)



- [10] The Friction Reducing Effect of Square-Shaped Surface Textures under Lubricated Line - Contacts - An Experimental Study, Ping Lu , Robert J. K. Wood , M.G. Gee, L. Wang, W. Pfleging “Lubricants”, vol 4(3), pg 26, (2016)
- [11] Hydrodynamic lubrication of textured surfaces: A review of modelling techniques and key findings; D. Gropper, L. Wang and T. Harvey, Trib International vol 94, pg 509, (2016)
- [12] Some innovative surface texturing techniques for tribological purposes ;HL. Costa,IM. Hutchings, “Part J: Journal of Engineering Tribology”, vol 229 issue: 4, pg 429, (2014)
- [13] Effect of surface texturing on friction reduction between ceramic and steel materials under lubricated sliding contact; M. Wakudaa, Y. Yamauchi, S. Kanzaki, Y. Yasuda; “Wear” vol 254, Issues 3–4, pg 356, (2003)
- [14] Combined friction and wear reduction in a reciprocating contact through laser surface texturing; SC. Vladescu, AV. Olver, IG. Pegg, T. Reddyhoff, “Wear” vol 358, pg 51, (2016)
- [15] Optimization of Pocket Geometry for Friction Reduction in Piston–Liner Contacts; SC. Vladescu, A. Ciniero, K. Tufail, A. Gangopadhyay, T. Reddyhoff “Tribology Transactions”, pg 1, (2017)
- [16] Lubricant film thickness and friction force measurements in a laser surface textured reciprocating line contact simulating the piston ring–liner pairing; SC. Vladescu, S. Medina, AV. Olver, IG. Pegg , T. Reddyhoff; “Tribology International” vol 98, pg 317, (2016)
- [17] Different aspects of the role of wear debris in fretting wear, M. Varenberg, G. Halperin, I. Etsion, “Wear” vol 252, pg 902, (2002)
- [18] Friction reduction under mixed and full film EHL induced by hot micro-coined surface patterns; A. Rosenkranza, A. Szurdak, C. Gachot, G. Hirt, F. Mucklich “Tribology International” vol 95, pg 290, (2016)
- [19] Effect of surface texturing on elasto hydrodynamically lubricated contact under transient speed conditions; I. Krupkaa, M. Hartl, M. Zimmerman, P. Houska, S. Jang; “Tribology International” vol 44, Issue 10, pg 1144, (2011)
- [20] Effectiveness and design of surface texturing for different lubrication regimes ;B. Podgornik, L.M. Vilhena, M. Sedlacek, Z. Rek, I. Zun ; “Meccanica” vol 47, pg 1613, (2012)
- [21] Microlubrication effect by laser-textured steel surfaces; P. Andersson, J. Koskinen, S. Varjus, Y. Gerbig, H. Haefke, S. Georgiou, B. Zhmud, W. Buss, “Wear” vol 262, Issues 3–4, pg 369, (2007)
- [22] The effect of damage accumulation behaviour on ablation thresholds and damage morphology in ultrafast laser micromachining of common metals in air; P.T. Mannion, J. Magee, E. Coyne, G.M. O’Connor, T. J. Glynn, “Appl. Surf. Sci.” vol 233, Issue (1–4), pg 275, (2004).
- [23] Laser-induced damage on single-crystal metal surfaces; Y. Jee, M. F. Becker, and R. M. Walser; “J. Opt. Soc. Am. B” vol 5(3), pg 648, (1988).
- [24] The effect of laser surface texturing on transitions in lubrication regimes during unidirectional sliding contact; A. Kovalchenkoa, O. Ajayia, A. Erdemir, G. Fenske, I. Etsion; “Tribology International” vol 38, Issue 3, pg 219, (2005)
- [25] K.L. Johnson, Contact Mechanics, Cambridge University Press, (1985)

[26] Contact of a rotating wheel with a flat;  
A. Sackfield, D. Dini , D.A. Hills;  
“International Journal of Solids and  
Structures” vol 44 pg 3304, (2007).